

Going beyond Local Density and Gradient Corrected XC functionals in Quantum-ESPRESSO



Jacob's ladder of Density Functional Theory

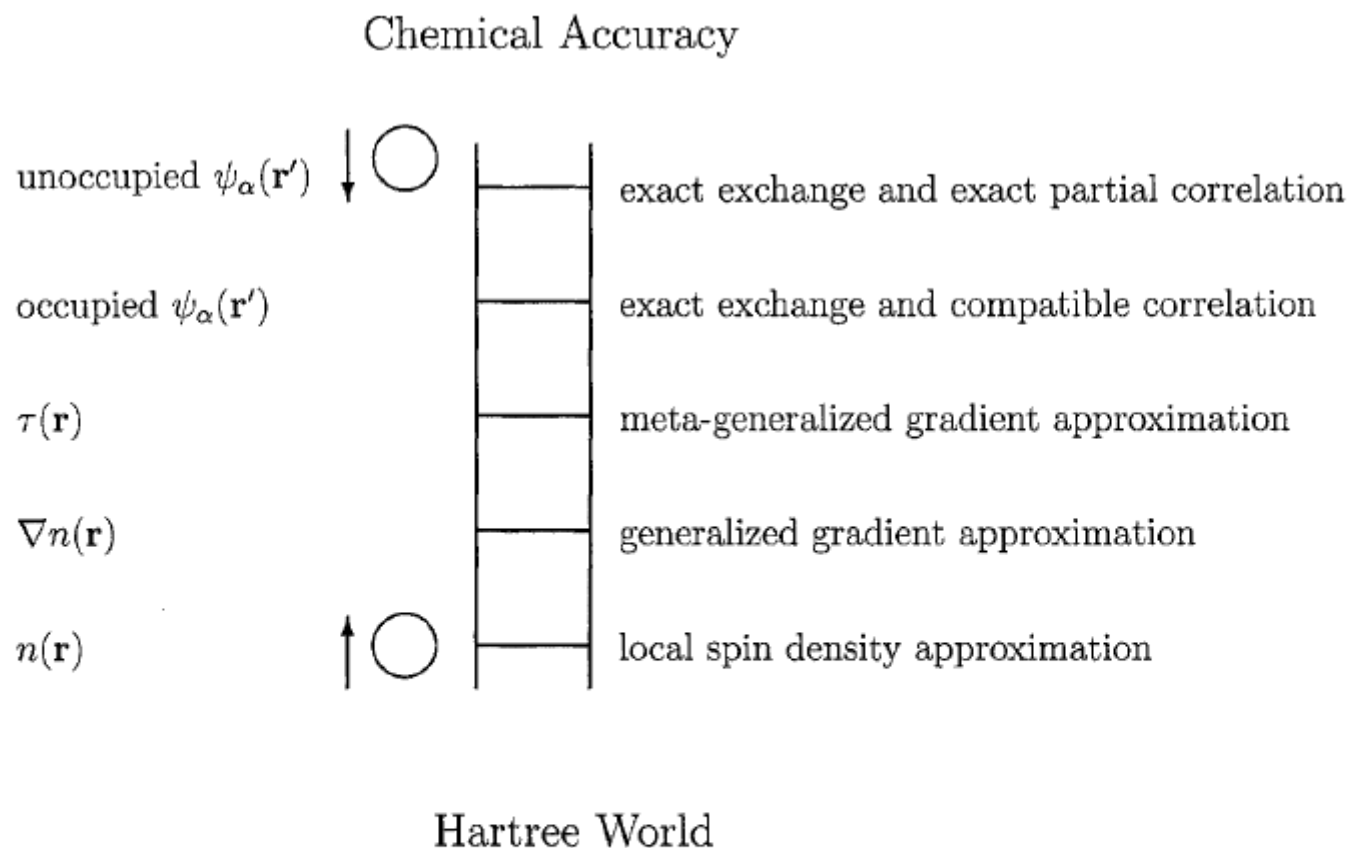


FIGURE 1. Jacob's ladder of density functional approximations. Any resemblance to the Tower of Babel is purely coincidental. Also shown are angels in the spherical approximation, ascending and descending. Users are free to choose the rungs appropriate to their accuracy requirements and computational resources. However, at present their safety can be guaranteed only on the two lowest rungs.

LDA and LSDA

GGA : PW91, PBE, revPBE, RPBE, BLYP

META-GGA: PKZB, TPSS,

SIC, DFT+U, hybrids

van der Waals functionals

...

exact DFT



LDA and LSDA



GGA : PW91, PBE, revPBE, RPBE, BLYP



~~META GGA: PKZB, TPSS,~~

~~SIC, DFT+U, hybrids~~

Van der Waals functionals

...

exact DFT



simple approximations can work reasonably

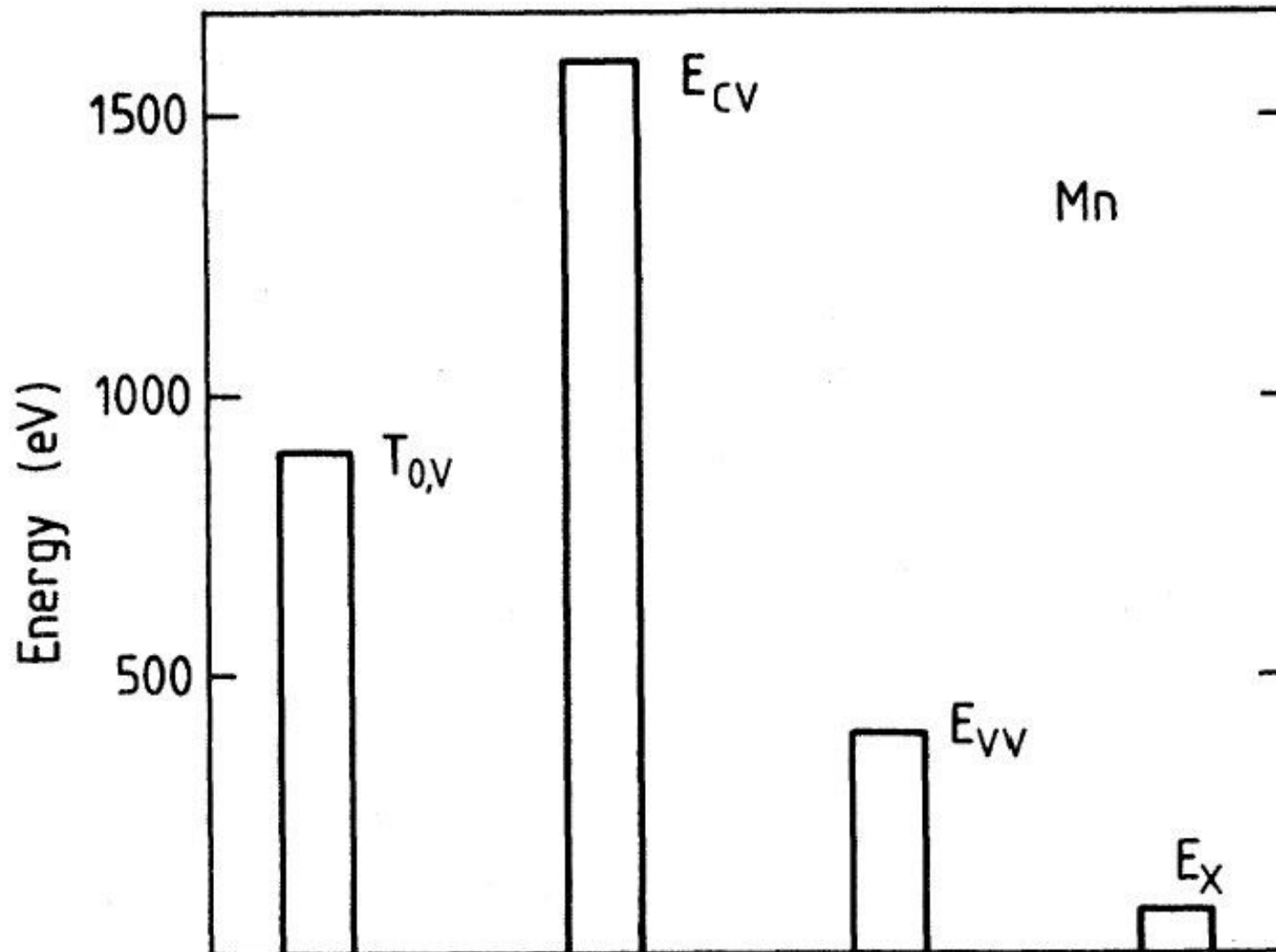


FIG. 4. Relative magnitudes of contributions to total valence energy of Mn atom (in eV).



simple approximations can work reasonably

L(S)DA

$$E_{XC}^{LSD}[n_{\uparrow}, n_{\downarrow}] = \int d^3 r n \epsilon_{XC}^{unif}(n_{\uparrow}, n_{\downarrow})$$

GGA

$$E_{XC}^{GGA}[n_{\uparrow}, n_{\downarrow}] = \int d^3 r f(n_{\uparrow}, n_{\downarrow}, \nabla n_{\uparrow}, \nabla n_{\downarrow})$$

Summary of Geometry Prediction

LDA under-predicts bond lengths (always ?)

GGA error is less systematic though over-prediction is common.

errors are in many cases $< 1\%$, for transition metal oxides $< 5\%$



Elemental Crystal Structures: GGA pseudopotential method

method

experimentally found to be fcc

experimentally found to be bcc

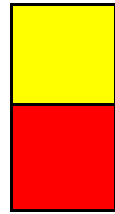
H																				
-0.12																				
Li	Bc															B	C	N	O	F
0.13	2.19															34.77	-19.71	-21.12	10.24	-4.53
0.11	0.04																-6.00			
0.11	0.50																			
Na	Mg															Al	Si	P	S	Cl
0.12	1.37															9.21	-1.89	-16.04	-17.63	-4.46
0.05	0.50															10.08	-4.00	7.95		
0.05	0.50															10.08	-4.00			
		VASP-PAW																		
		SGTE data																		
		Saunders et al																		
K	Ca	Sc	Ti	V	Cr	Mn	Fe	Co	Ni	Cu	Zn	Ga	Ge	As	Se	Br				
0.04	1.64	5.80	4.79	-23.95	-36.76	7.41	-8.45	8.36	9.23	2.84	5.94	1.48	0.70	-10.71	-14.67	-2.85				
-0.05	1.41	-3.02	0.48	-7.50	-8.13	0.78	-7.97	1.71	7.99	4.02	-0.08	0.70	-1.90							
-0.05	0.93			-15.30	-9.19	1.80		4.20	7.49	4.02	6.03	0.70	-1.90							
Rb	Sr	Y	Zr	Nb	Mo	Tc	Ru	Rh	Pd	Ag	Cd	In	Sn	Sb	Te	I				
0.08	0.43	10.02	3.61	-31.20	-38.74	19.04	48.93	32.39	3.74	2.27	4.90	1.02	0.99	-8.96	-11.19	-1.26				
-0.20	1.33	1.19	-0.29	-13.50	-15.20	8.00	9.00	19.00	10.50	3.40		0.64	-1.11							
-0.20	0.75			-22.00	-28.00	8.00	14.00	19.00	10.50	3.40		0.65	0.25							
Cs	Ba			Hf	Ta	W	Re	Os	Ir	Pt	Au	Hg	Tl	Pb	Bi	Po	At			
0.10	-1.62			10.14	-23.75	-45.03	24.87	70.92	59.39	7.85	1.90	-1.02	-1.40	4.06	-4.53					
-0.50	-1.80			2.38	-16.00	-19.30	6.00	14.50	32.00	15.00	4.25		-0.09	2.40	1.40					
-0.50	-1.80			-4.14	-26.50	-33.00	18.20	30.50	32.00	15.00	4.25		0.07	2.40						
		La	Ce	Pr	Nd	Pm	Sm	Eu	Gd	Tb	Dy	Ho	Er	Tm	Yb	Lu				
		12.22	22.40	11.55	11.99	12.55	12.88	-1.61	13.11	12.97	12.73	12.36	11.86			9.91				
Fr	Ra	Ac	Th	Pa	U	Np	Pu	Am	Cm	Bk	Cf	Es	Fm	Md	No	Lr				
		12.56	13.95	17.09	-10.36	-23.17	11.73													

data taken from:

Y. Wang,^a S. Curtarolo,^{et al.} *Ab Initio Lattice Stability in Comparison with CALPHAD Lattice Stability*, Computer Coupling of Phase Diagrams and Thermochemistry (Calphad) Vol. 28, Issue 1, March 2004, Pages 79-90.



Elemental Crystal Structures: GGA pseudopotential method



experimentally found to be hcp

experimentally found to be fcc

$$E_{\text{hcp}} - E_{\text{fcc}} \text{ (kJ/mole)}$$

H -0.01												B -78.73	C -6.18 -3.00	N -34.15	O 1.00	F -14.64	
Li 0.19 -0.05 -0.05	Be -7.91 -8.35 -6.35												Al 2.85 5.48 3.48	Si -3.26 -1.80 -1.80	P -3.77	S -43.63	Cl -16.81
Na 0.06 -0.05 -0.05	Mg -1.22 -2.60 -2.60	←←← VASP-PAW SGTE data Saunders et al →→→															
K 0.26 0.00	Ca 0.31 0.50 0.50	Sc -4.48 -5.00	Ti -5.51 -6.00 -6.00	V 0.53 -3.50 -4.80	Cr 0.91 -2.85 -1.82	Mn -3.01 -1.00 -1.00	Fe -7.76 -2.24	Co -1.95 -0.43 -0.43	Ni 2.22 2.89 1.50	Cu 0.32 0.60 0.60	Zn -0.79 -2.97	Ga 0.69 0.70 0.70	Ge -0.28 -1.00 -1.00	As -4.83	Se -35.43	Br 3.00	
Rb -0.01 0.00	Sr 0.38 0.25 0.25	Y -2.13 -6.00	Zr -3.69 -7.60 -7.60	Nb -3.08 -3.50 -5.00	Mo 1.14 -3.65 -5.00	Tc -6.53 -10.00 -10.00	Ru -10.79 -12.50 -12.50	Rh 3.26 3.00 3.00	Pd 2.50 2.00 2.00	Ag 0.29 0.30 0.30	Cd -1.00 -0.89	In 0.35 0.37 0.65	Sn -0.50 -1.61 -0.25	Sb -3.94	Te 23.40	I 0.99	
Cs -0.06 0.00	Ba -0.40 0.20 0.20		Hf -6.82 -10.00 -10.00	Ta 3.06 -4.00 -6.50	W -1.79 -4.55 -6.00	Re -6.26 -11.00 -11.00	Os -13.26 -13.00 -13.00	Ir 6.55 4.00 4.00	Pt 5.02 2.50 2.50	Au 0.08 0.24 0.55	Hg -1.51 -2.07	Tl -1.80 -0.31 -0.31	Pb 1.80 0.30 0.30	Bi -4.03	Po	At	
		La 2.63	Ce 8.50	Pr 2.07	Nd 1.94	Pm 1.77	Sm 1.53	Eu 0.24	Gd 0.77	Tb 0.24	Dy -0.41	Ho -1.18	Er -1.97	Tm	Yb	Lu -3.85	
Fr	Ra	Ac 0.93	Th 4.00	Pa 0.49	U -15.79	Np -14.01	Pu 0.69	Am	Cm	Bk	Cf	Es	Fm	Md	No	Lr	

data taken from:

Y. Wang,¹ S. Curtarolo,^{2*} *Ab Initio Lattice Stability in Comparison with CALPHAD Lattice Stability*, Computer Coupling of Phase Diagram and Thermochemistry (Calphad) Vol. 28, Issue 1, March 2004, Pages 79-90.



Summary: Comparing Energy of Structures

For most elements, both LDA and GGA predict the correct structure for a material (as far as we know)

Notable exceptions: Fe in LDA; materials with substantial electron correlation effects (e.g. Pu)



Redox Reactions can be more Problematic



GGA

2.8 eV

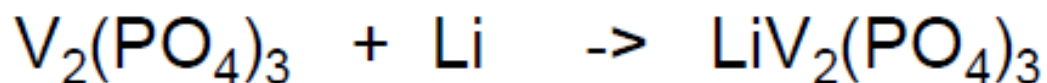
Exp

3.5 eV



3.6 eV

4.1 eV



3.3 eV

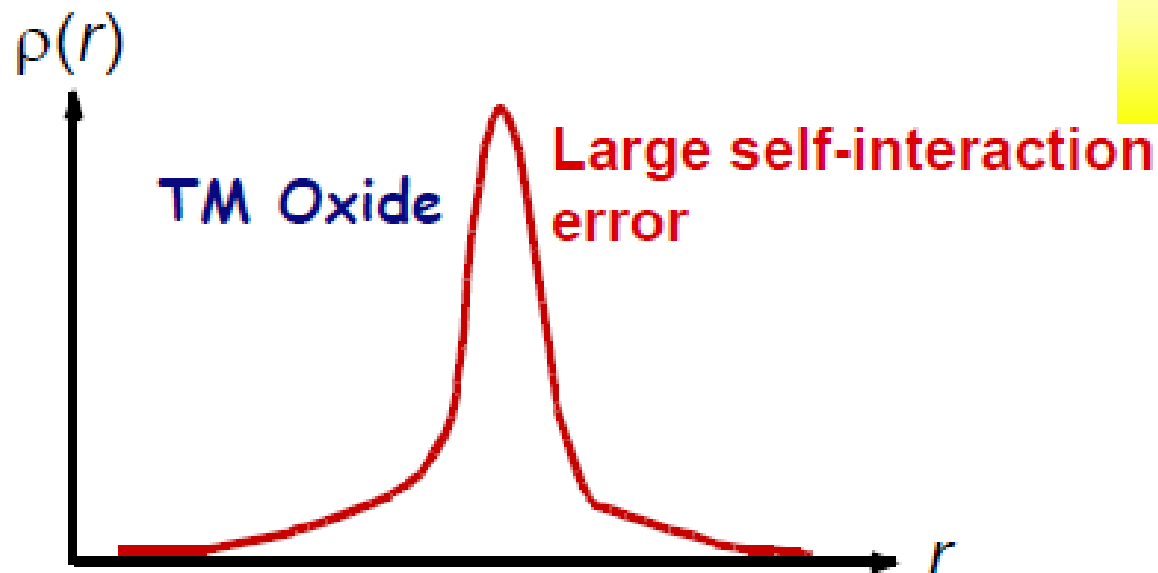
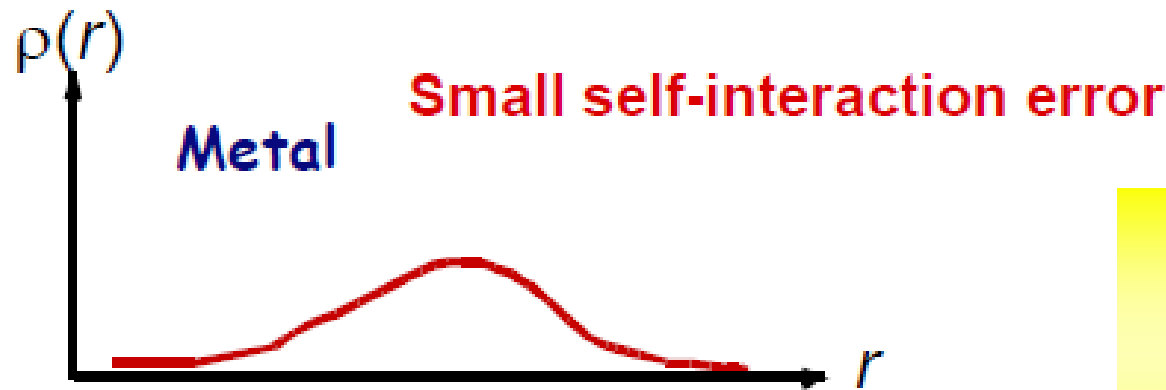
4.6 eV

All these reactions involve the transfer of an electron from a delocalized state in Li metal to a localized state in the transition metal oxide (phosphate)



In standard DFT an electron interacts with the effective potential generated by all the electrons (including itself)

$$H = \sum_i H_i = \sum_{i=1}^{N_e} \nabla_i^2 + \sum_{i=1}^{N_e} V_{nuclear}(r_i) + \sum_{i=1}^{N_e} V_{effective}(r_i)$$



**Self interaction in DFT
is key problem in transition
metal oxides**

Problems with LDA / GGA functionals

- Chemical accuracy (1 kcal/mol) is far.
 - trends are often accurate for strong bonds (covalent, ionic, metallic)
 - weak bonds/small overlaps are problematic
- Self interaction cancellation is only approximately verified in LDA and GGA.
 - molecular dissociation limit, TMO & RE and other atom-in-solid system.
- van der Waals interactions are not taken into account
 - occasional agreement with exp. from compensation of errors



Problems with LDA / GGA functionals

- Chemical accuracy (1 kcal/mol) is far.
 - trends are often accurate for strong bonds (covalent, ionic, metallic)
 - weak bonds/small overlaps are problematic
- Self interaction cancellation is only approximately verified in LDA and GGA.
 - molecular dissociation limit, TMO & RE and other atom-in-solid system.
- van der Waals interactions are not taken into account
 - occasional agreement with exp. from compensation of errors



SIC, DFT+U, hybrids

Self interaction correction was proposed as early as in 1981 by Perdew-Zunger. Conceptually important but not widely used.

DFT+U has been introduced by Anisimov, Zaanen and Andersen as an approximation to treat strongly correlated materials. It has been more recently been applied also in more normal system with encouraging results.

Hybrid functionals (like PBE0, B3LYB) mix a fraction of Self-interaction-free HF with LDA/GGA functionals.
Is the method preferred by chemists.
It is very expensive in a plane-wave basis.



Derivation

Full-Interacting Hamiltonian

$$H = T + W + v_{\text{ext}} \Rightarrow |\Psi^{\text{GS}}\rangle, n(\mathbf{r})$$

Non-Interacting (Kohn-Sham) Hamiltonian

$$H_{\text{KS}} = T_s + v_{\text{KS}} \Rightarrow |\Phi_{\text{KS}}^{\text{GS}}\rangle, n(\mathbf{r})$$

then we introduce fictitious systems with **scaled interaction** λW which connect the KS ($\lambda = 0$) with the Many-Body system ($\lambda = 1$)

Adiabatic Connection

$$H_\lambda = T + \lambda W + v_{\text{ext}}^\lambda$$

$$v_{\text{ext}}^{\lambda=0} = v_{\text{KS}}$$

$$v_{\text{ext}}^{\lambda=1} = v_{\text{ext}}$$

$$n_\lambda(\mathbf{r}) = \langle \Psi_\lambda^{\text{GS}} | \hat{n}(\mathbf{r}) | \Psi_\lambda^{\text{GS}} \rangle = n(\mathbf{r})$$

Derivation

According to **Hellmann-Feynman** theorem

$$\frac{dE_\lambda}{d\lambda} = \langle \Psi_\lambda | \frac{dH_\lambda}{d\lambda} | \Psi_\lambda \rangle = \langle \Psi_\lambda | W | \Psi_\lambda \rangle + \langle \Psi_\lambda | \frac{\partial v_{\text{ext}}}{\partial \lambda} | \Psi_\lambda \rangle$$

Integrating over λ between 0 and 1

$$E_{\lambda=1} = E_{\lambda=0} + \int_0^1 d\lambda \langle \Psi_\lambda | W | \Psi_\lambda \rangle + \int d\mathbf{r} n(\mathbf{r}) [v_{\text{ext}}(\mathbf{r}) - v_{\text{KS}}(\mathbf{r})]$$

With the usual decomposition of energy functional

$$E_{\lambda=1} = T_s + E_H + E_{\text{xc}} + \int d\mathbf{r} n(\mathbf{r}) v_{\text{ext}}(\mathbf{r})$$

$$E_{\lambda=0} = T_s + \int d\mathbf{r} n(\mathbf{r}) v_{\text{KS}}(\mathbf{r})$$

we end up with

$$E_H + E_{\text{xc}} = \int_0^1 d\lambda \langle \Psi_\lambda | W | \Psi_\lambda \rangle$$

Hartree-Fock energy

$$\mathbf{E}_{HF} = -\frac{e^2}{2} \sum_{\substack{\mathbf{k}v \\ \mathbf{k}'v'}} \int \frac{\phi_{\mathbf{k}v}^*(\mathbf{r})\phi_{\mathbf{k}'v'}(\mathbf{r})\phi_{\mathbf{k}'v'}^*(\mathbf{r}')\phi_{\mathbf{k}v}(\mathbf{r}')}{|\mathbf{r} - \mathbf{r}'|} d\mathbf{r}d\mathbf{r}'$$

- Hartree-Fock
- Exact Exchange (OEP)
- Hybrid Functionals: HH, B3LYP, PBE0
(range separated) HSE

HF Vx using PWs

- FFT pseudo wfc to real space

$$\phi_{\mathbf{k}v}(\mathbf{k} + \mathbf{G}) \xrightarrow{FFT} \phi_{\mathbf{k}v}(\mathbf{r})$$

- For each qpoint and each occupied band build “charge density”

$$\rho_{\mathbf{q}}(\mathbf{r}) = \phi_{\mathbf{k}-\mathbf{q}v'}^*(\mathbf{r}) \phi_{\mathbf{k}v}(\mathbf{r})$$

- FFT charge to recip.space and solve Poisson eq.

$$\rho_{\mathbf{q}}(\mathbf{r}) \xrightarrow{FFT} \rho_{\mathbf{q}}(\mathbf{q} + \mathbf{G}) \implies V_{\mathbf{q}}(\mathbf{q} + \mathbf{G}) = \frac{4\pi e^2}{|\mathbf{q} + \mathbf{G}|^2} \rho_{\mathbf{q}}(\mathbf{q} + \mathbf{G})$$

- FFT back to real space, multiply by wfc and add to result

$$V_{\mathbf{q}}(\mathbf{q} + \mathbf{G}) \xrightarrow{FFT} V_{\mathbf{q}}(\mathbf{r}) \implies V_x \phi_{\mathbf{k}v}(\mathbf{r}) = V_x \phi_{\mathbf{k}v}(\mathbf{r}) + \phi_{\mathbf{k}-\mathbf{q}v'}(\mathbf{r}) V_{\mathbf{q}}(\mathbf{r})$$



The $\mathbf{q}+\mathbf{G}=0$ divergence

- Gygi-Baldereschi PRB 34, 4405 (1986)

$$\rho_{\mathbf{k}-\mathbf{q},v'}(\mathbf{r}) = \phi_{\mathbf{k}-\mathbf{q},v'}^*(\mathbf{r})\phi_{\mathbf{k},v}(\mathbf{r}) \quad \Rightarrow \quad A(\mathbf{q} + \mathbf{G}) = \frac{\Omega}{(2\pi)^3} \int d\mathbf{k} |\rho_{\mathbf{k},v}^{\mathbf{k}-\mathbf{q},v'}(\mathbf{q} + \mathbf{G})|^2$$
$$= \frac{1}{N_{\mathbf{k}}} \sum_{\mathbf{k}} |\rho_{\mathbf{k},v}^{\mathbf{k}-\mathbf{q},v'}(\mathbf{q} + \mathbf{G})|^2$$

$$E_{HF} = -\frac{4\pi e^2}{2\Omega} \times \frac{\Omega}{(2\pi)^3} \int d\mathbf{q} \sum_{\mathbf{G}} \frac{A(\mathbf{q} + \mathbf{G})}{|\mathbf{q} + \mathbf{G}|^2}$$

integrable divergence

The $\mathbf{q}+\mathbf{G}=0$ divergence

- Gygi-Baldereschi PRB 34, 4405 (1986)

$$\rho_{\mathbf{k}-\mathbf{q},v'}(\mathbf{r}) = \phi_{\mathbf{k}-\mathbf{q},v'}^*(\mathbf{r})\phi_{\mathbf{k},v}(\mathbf{r}) \quad \Rightarrow \quad A(\mathbf{q} + \mathbf{G}) = \frac{\Omega}{(2\pi)^3} \int d\mathbf{k} |\rho_{\mathbf{k},v}^{\mathbf{k}-\mathbf{q},v'}(\mathbf{q} + \mathbf{G})|^2$$
$$= \frac{1}{N_{\mathbf{k}}} \sum_{\mathbf{k}} |\rho_{\mathbf{k},v}^{\mathbf{k}-\mathbf{q},v'}(\mathbf{q} + \mathbf{G})|^2$$

$$E_{HF} = -\frac{4\pi e^2}{2\Omega} \times \left\{ \frac{\Omega}{(2\pi)^3} \int d\mathbf{q} \sum_{\mathbf{G}} \frac{A(\mathbf{q} + \mathbf{G}) - A(0)e^{-\alpha|\mathbf{q}+\mathbf{G}|^2}}{|\mathbf{q} + \mathbf{G}|^2} + \frac{\Omega}{(2\pi)^3} \int d\mathbf{q} \sum_{\mathbf{G}} \frac{e^{-\alpha|\mathbf{q}+\mathbf{G}|^2}}{|\mathbf{q} + \mathbf{G}|^2} A(0) \right\}$$

The $\mathbf{q}+\mathbf{G}=0$ divergence

- Gygi-Baldereschi PRB 34, 4405 (1986)

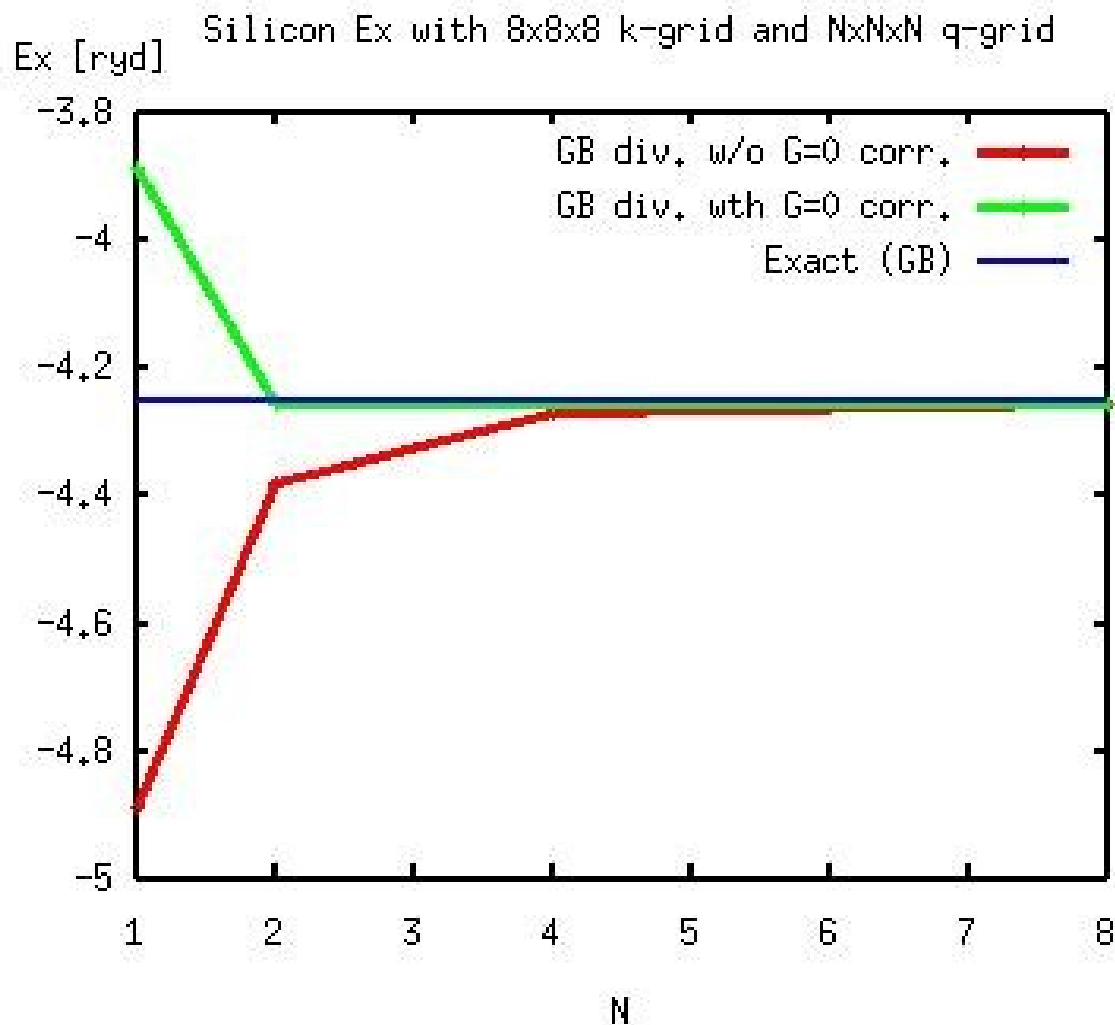
$$\rho_{\mathbf{k}-\mathbf{q},v'}(\mathbf{r}) = \phi_{\mathbf{k}-\mathbf{q},v'}^*(\mathbf{r})\phi_{\mathbf{k},v}(\mathbf{r}) \quad \Rightarrow \quad A(\mathbf{q} + \mathbf{G}) = \frac{\Omega}{(2\pi)^3} \int d\mathbf{k} |\rho_{\mathbf{k},v}^{\mathbf{k}-\mathbf{q},v'}(\mathbf{q} + \mathbf{G})|^2$$

$$= \frac{1}{N_{\mathbf{k}}} \sum_{\mathbf{k}} |\rho_{\mathbf{k},v}^{\mathbf{k}-\mathbf{q},v'}(\mathbf{q} + \mathbf{G})|^2$$

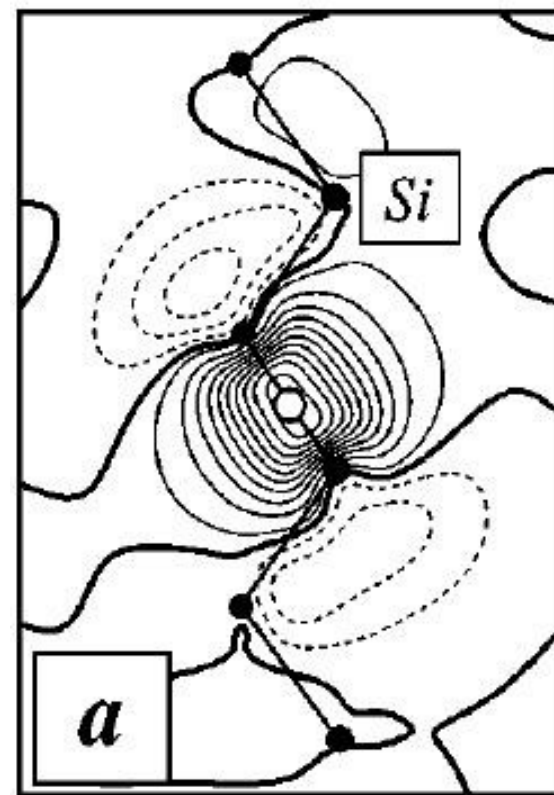
$$E_{HF} = -\frac{4\pi e^2}{2\Omega} \times \left\{ \frac{1}{N_{\mathbf{q}}} \left[\sum'_{\mathbf{q},\mathbf{G}} \frac{A(\mathbf{q} + \mathbf{G})}{|\mathbf{q} + \mathbf{G}|^2} + \lim_{\mathbf{q} \rightarrow 0} \frac{A(\mathbf{q}) - A(0)}{\mathbf{q}^2} \right] + D \times A(0) \right\}$$

$$D = \frac{1}{N_{\mathbf{q}}} \left[-\sum'_{\mathbf{q},\mathbf{G}} \frac{e^{-\alpha|\mathbf{q}+\mathbf{G}|^2}}{|\mathbf{q} + \mathbf{G}|^2} + \alpha \right] + \frac{\Omega}{(2\pi)^3} \sqrt{\frac{\pi}{\alpha}}$$

Silicon Bulk



F.Gygi, EPFL PhD thesis (1988)



Fernandez, Dal Corso,
Baldereschi,
PRB 58, R7480 (1998)

Simple Molecules

	HF		PW	PBE		PW	PBE0		EXP
	PW	G		PAW	G		PAW	G	
N_2	114	115	239	244	244	221	225	226	227
O_2	36	33	139	143	144	121	124	125	118
CO	173	175	265	269	269	252	255	256	261

PAW : Paier,Hirschl,Marsman and Kresse, J. Chem. Phys. 122, 234102 (2005)

Energies in kcal/mol = 43.3 meV



Scaling

- Kinetic energy and local Potential

$$NPW + 2 * FFT + NRXX$$

- Non local potential

$$2 * NBND * NPW$$

- Fock operator

$$2 * FFT + NBND * NQ * (NRXX + FFT) + 2 * NRXX$$

Scaling

- Kinetic energy and local Potential

$$NPW + 2 * FFT + NRXX$$

- Non local potential

$$2 * NBND * NPW$$

- Fock operator

$$2 * FFT + NBND * NQ * (NRXX + FFT) + 2 * NRXX$$

From 10 to 100 times slower than standard case

Scaling

- Kinetic energy and local Potential

$$NPW + 2 * FFT + NRXX$$

- Non local potential

$$2 * NBND * NPW$$

- Fock operator

$$2 * FFT + NBND * NQ * (NRXX + FFT) + 2 * NRXX$$

From 10 to 100 times slower than standard case

Moore's law: computer power doubles every 18 months
(a factor of 10 in 5 yrs)



Scaling

- Kinetic energy and local Potential

$$NPW + 2 * FFT + NRXX$$

- Non local potential

$$2 * NBND * NPW$$

- Fock operator

$$2 * FFT + NBND * NQ * (NRXX + FFT) + 2 * NRXX$$

From 10 to 100 times slower than standard case

Separation of long- and short-range part in X can help



the modified scf cycle

The HF energy is

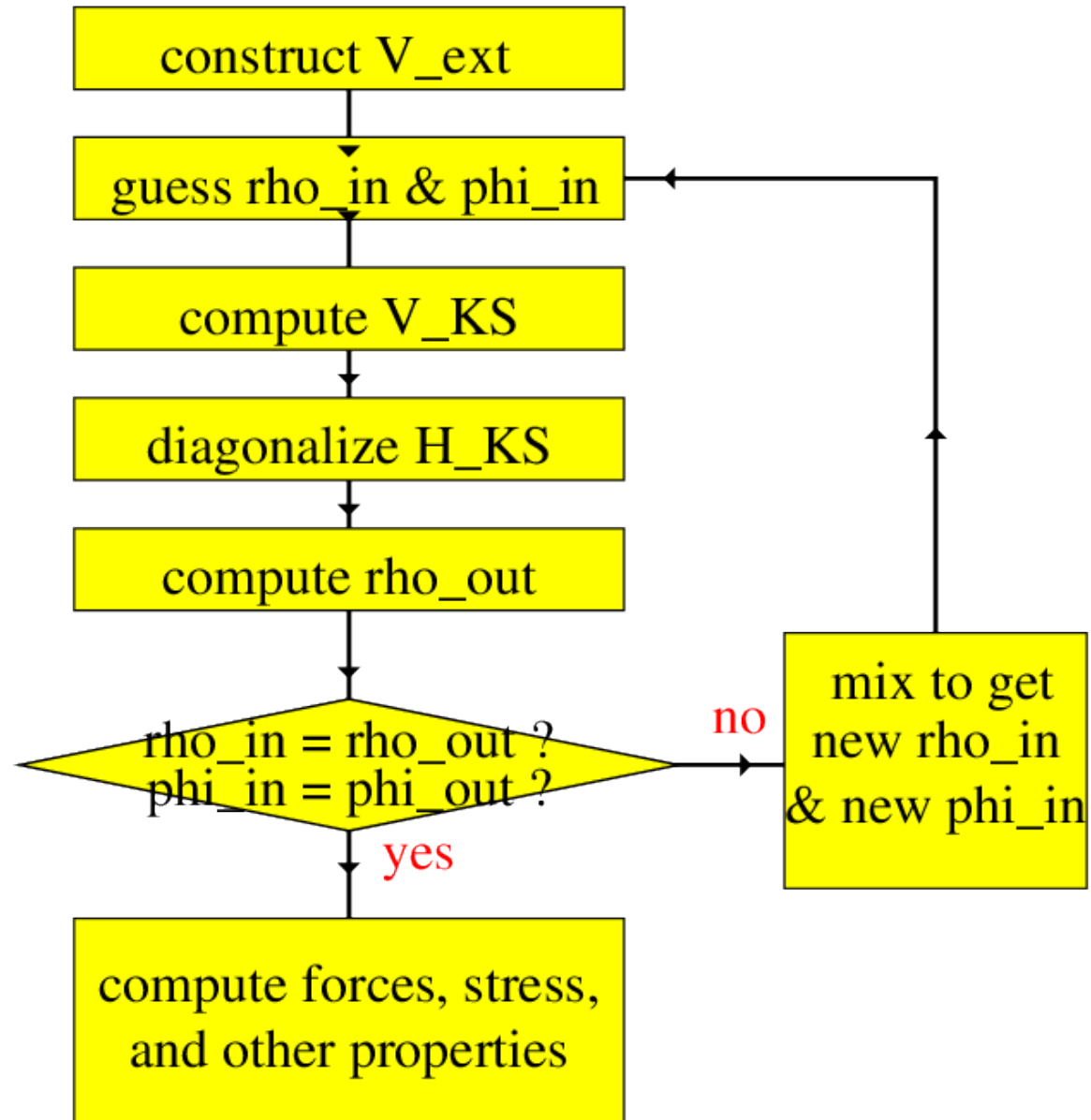
$$E_{HF}[\Phi] = \sum_i \langle \phi_i | -\frac{\hbar^2}{2m} \nabla^2 | \phi_i \rangle + \int V_{ext}(r) \rho(r) dr + E_H[\rho] + E_{WLD} - \frac{e^2}{2} \int \frac{|\gamma_\phi(r, r')|^2}{|r - r'|}$$

$$\text{with } \gamma_\phi(r, r') = \sum_i \phi_i(r) \phi_i^*(r')$$

The HF equations are therefore

$$\left[-\frac{\hbar^2}{2m} \nabla^2 + V_{ext}(r) + V_H(r) - e^2 \int \frac{\gamma_\phi(r, r')}{|r - r'|} \right] | \phi_i \rangle = \varepsilon_i | \phi_i \rangle$$

the modified scf cycle



the modified scf cycle

Let's introduce an auxiliary set of functions

$$E_{HF}[\Phi, \Psi] = \sum_i \langle \phi_i | -\frac{\hbar^2}{2m} \nabla^2 | \phi_i \rangle + \int V_{ext}(r) \rho(r) dr + E_H[\rho] + E_{WL} \\ - \frac{e^2}{2} \int \frac{|\gamma_\phi(r, r')|^2}{|r - r'|} + \frac{e^2}{2} \int \frac{|\gamma_\phi(r, r') - \gamma_\psi(r, r')|^2}{|r - r'|}$$

delta_exx > 0 !

with $\gamma_\phi(r, r') = \sum_i \phi_i(r) \phi_i^*(r')$, $\gamma_\psi(r, r') = \sum_i \psi_i(r) \psi_i^*(r')$

the modified scf cycle

Let's introduce an auxiliary set of functions

$$E_{HF}[\Phi, \Psi] = \sum_i \langle \phi_i | -\frac{\hbar^2}{2m} \nabla^2 | \phi_i \rangle + \int V_{ext}(r) \rho(r) dr + E_H[\rho] + E_{WL} \\ - \frac{e^2}{2} \int \frac{|\gamma_\phi(r, r')|^2}{|r - r'|} + \frac{e^2}{2} \int \frac{|\gamma_\phi(r, r') - \gamma_\psi(r, r')|^2}{|r - r'|}$$



$$E_X^{HF}[\Phi] - E_X^{HF}[\Phi] + \sum_i \langle \phi_i | V_X^{HF}[\Psi] | \phi_i \rangle - E_X^{HF}[\Psi]$$

with $\gamma_\phi(r, r') = \sum_i \phi_i(r) \phi_i^*(r')$, $\gamma_\psi(r, r') = \sum_i \psi_i(r) \psi_i^*(r')$

the modified scf cycle

Let's introduce an auxiliary set of functions

$$E_{HF}[\Phi, \Psi] = \sum_i \langle \phi_i | -\frac{\hbar^2}{2m} \nabla^2 | \phi_i \rangle + \int V_{ext}(r) \rho(r) dr + E_H[\rho] + E_{WL} \\ - \frac{e^2}{2} \int \frac{|\gamma_\phi(r, r')|^2}{|r - r'|} + \frac{e^2}{2} \int \frac{|\gamma_\phi(r, r') - \gamma_\psi(r, r')|^2}{|r - r'|}$$



$$\cancel{E_X^{HF}[\Phi]} - \cancel{E_X^{HF}[\Phi]} + \sum_i \langle \phi_i | V_X^{HF}[\Psi] | \phi_i \rangle - E_X^{HF}[\Psi]$$

with $\gamma_\phi(r, r') = \sum_i \phi_i(r) \phi_i^*(r')$, $\gamma_\psi(r, r') = \sum_i \psi_i(r) \psi_i^*(r')$

the modified scf cycle

Let's introduce an auxiliary set of functions

$$E_{HF}[\Phi, \Psi] = \sum_i \langle \phi_i | -\frac{\hbar^2}{2m} \nabla^2 | \phi_i \rangle + \int V_{ext}(r) \rho(r) dr + E_H[\rho] + E_{WL} \\ + \sum_i \langle \phi_i | V_X^{HF}[\Psi] | \phi_i \rangle - E_X^{HF}[\Psi]$$

with $\gamma_\phi(r, r') = \sum_i \phi_i(r) \phi_i^*(r')$, $\gamma_\psi(r, r') = \sum_i \psi_i(r) \psi_i^*(r')$

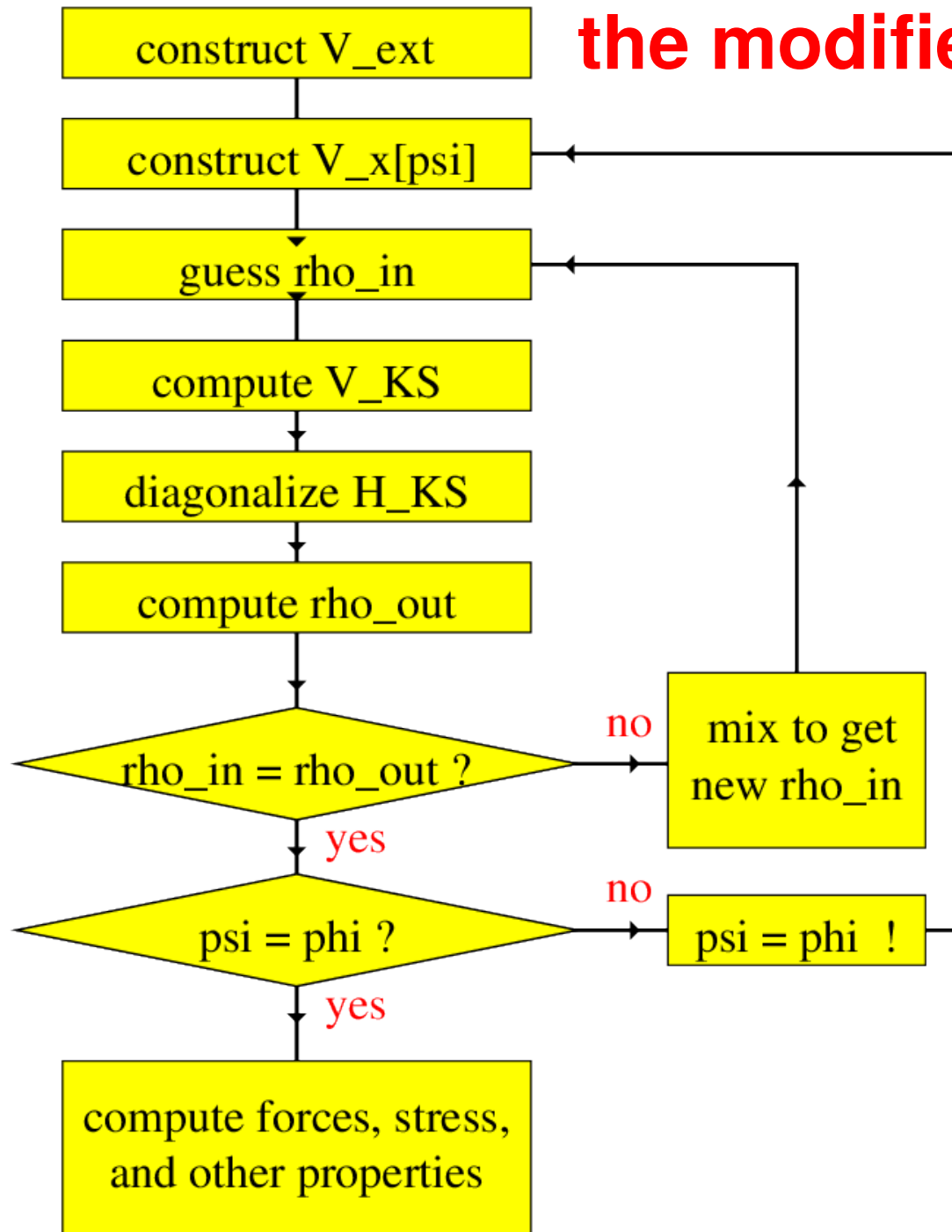
The minimizing equations become

$$\left[-\frac{\hbar^2}{2m} \nabla^2 + V_{ext}(r) + V_H(r) - e^2 \int \frac{\gamma_\psi(r, r')}{|r-r'|} \right] |\phi_i\rangle = \varepsilon_i |\phi_i\rangle$$

and $\psi_i(r) = \phi_i(r), \forall i$



the modified scf cycle



Adaptively Compressed Exchange (ACE)

Applying the Fock operator is extremely expensive !



Adaptively Compressed Exchange (ACE)

Applying the Fock operator is extremely expensive !

One can try to approximate it via a KB-type factorization in the inner loop of the nested scf-cycle (ACE)

$$V_X^{HF}[\Psi] \approx \sum_{i,j} |w_i\rangle a_{ij} \langle w_j|$$

such that it works exactly on the reference wfc $|\psi_k\rangle$



Adaptively Compressed Exchange (ACE)

Applying the Fock operator is extremely expensive !

One can try to approximate it via a KB-type factorization in the inner loop of the nested scf-cycle (ACE)

$$V_X^{HF}[\Psi] \approx \sum_{i,j} |w_i\rangle a_{ij} \langle w_j|$$

such that it works exactly on the reference wfc $|\psi_k\rangle$

$$|w_k\rangle = V_X^{HF}[\Psi]|\psi_k\rangle \Rightarrow |w_k\rangle = \sum_{i,j} |w_i\rangle a_{ij} \langle \psi_j| V_X^{HF}[\Psi]|\psi_k\rangle$$

$$\sum_j a_{ij} \langle \psi_j| V_X^{HF}[\Psi]|\psi_k\rangle = \delta_{i,k}$$

$$\Rightarrow a_{ij} = \langle \psi| V_X^{HF}[\Psi]|\psi\rangle_{ij}^{-1}$$



Adaptively Compressed Exchange (ACE)

Applying the Fock operator is extremely expensive !

One can try to approximate it via a KB-type factorization in the inner loop of the nested scf-cycle (ACE)

$$V_X^{HF}[\Psi] \approx \sum_{i,j} |w_i\rangle a_{ij} \langle w_j|$$

such that it works exactly on the reference wfcs $|\psi_k\rangle$

$$|w_k\rangle = V_X^{HF}[\Psi]|\psi_k\rangle, \quad a_{ij} = \langle \psi | V_X^{HF}[\Psi] | \psi \rangle_{ij}^{-1}$$

in this way the calculation of H_ψ in the inner loop is comparable to a non-hybrid functional.

on the fully self-consistent wfcs the ACE operator is exact !



LDA and LSDA



GGA : PW91, PBE, revPBE, RPBE, BLYP



~~META GGA: PKZB, TPSS,~~

~~SIC, DFT+U, hybrids~~



van der Waals functionals

...

exact DFT



... to be continued